Measurement Science
and Technology

PAPER • **OPEN ACCESS**

Microwave WGM resonator with a capillary tube for the characterization of bioliquids

To cite this article: Alexey I Gubin *et al* 2025 *Meas. Sci. Technol.* **36** 105111

OPEN ACCESS
IOP Publishing
Measurement Science and Technology
Meas. Sci. Technol. **36** (2025) 105111 (8pp)
https://doi.org/10.1088/1361-6501/ae0e9f

Microwave WGM resonator with a capillary tube for the characterization of bioliquids

Alexey I Gubin[1,*], Irina A Protsenko[1], Alexander A Barannik[1], Alexandr A Lavrinovich[1] and Svetlana A Vitusevich[2]

[1] O.Ya. Usikov Institute for Radiophysics and Electronics NAS of Ukraine, Kharkiv, Ukraine
[2] Institute of Biological Information Processing (IBI-3), Forschungszentrum Jülich, Jülich, Germany

E-mail: gubin@ire.kharkov.ua

Received 17 April 2025, revised 21 September 2025
Accepted for publication 2 October 2025
Published 15 October 2025

Abstract

Microwave (MW) studies of biochemical liquids require the precise determination of permittivity and a convenient sample placement in a sterile channel, which must be cleaned or replaced after testing. These requirements can be effectively met using the proposed MW characterization technique. This technique is based on a high-quality whispering-gallery mode (WGM) quartz resonator. The liquid under test is filled in a capillary tube (CT), which is placed in the resonator hole. A calibration approach based on simulations for the extraction of complex permittivity values of biochemical liquids of sub-microliter volumes was demonstrated and successfully verified. This was achieved through a special procedure for the analysis of the interaction of the electromagnetic field with the liquid in a CT inside a WGM quartz resonator and measurements of its frequency response. The reliability of the technique was validated by simulation and the measurement of liquids with known characteristics. The approach was successfully applied to obtain the complex permittivity of glucose in water solutions in the Ka-band.

Supplementary material for this article is available online

Keywords: computer simulations, capillary tube, microwave measurement, permittivity, whispering gallery mode, dielectric resonator

1. Introduction

The investigation of liquid properties in the microwave (MW) range is vital in various fields of science and technology [1]. The MW dielectric permittivity characterization technique enables fast and label-free analysis using non-expensive equipment. Moreover, each substance is characterized by a unique complex permittivity value and its specific frequency dependence. Therefore, investigation in MW frequency range provide additional information for substance identification. There are a number of permittivity determination techniques in the MW range [2, 3]. All the methods can be categorized into resonance [4] and non-resonance [5, 6] techniques. In each case, the liquid is positioned in a structure in relation to the electromagnetic field pattern, where the liquid under test (LUT) properties influence this pattern. Analyzing the response of the electromagnetic field thus provides a way

* Author to whom any correspondence should be addressed.

of determining the liquid properties. The interaction between the LUT and the electromagnetic field is determined by the complex permittivity of the liquid, making this parameter a key characteristic in the MW range.

Both resonant and non-resonant methods are used to measure dielectric permittivity. Resonant methods generally offer higher accuracy and sensitivity with lower substance detection limits [4, 7–9] compared to non-resonant methods [5, 6, 10]. However, in liquids with high MW absorption, substantial energy losses occur during interaction with the field, making it challenging to perform accurate measurements. MW resonant methods make use of various resonant configurations, such as cavity [11, 12], split-ring [13–15], metamaterial split-ring [16], patch [17, 18], dielectric [8, 9] or transmission line [3] resonators. MW planar split-ring, metamaterial and patch antenna resonators are typically compact size portable sensors allowing investigation of small amounts of liquid with relatively high accuracy. The quality factor of such resonators usually ranges from tens to hundreds. However, methods utilizing different whispering gallery mode (WGM) resonators [8, 9, 19] provide even higher quality factors due to the confinement of the electromagnetic field near the inner wall of the resonator. The quality factor of WGM sapphire or quartz resonators with LUT is usually up to two orders of magnitude higher compared to split-ring resonators. The resulting higher accuracy and lower substance detection limit (higher sensitivity) make the WGM based approach particularly suitable compared to other resonant methods.

A crucial task, especially in the study of expensive DNA-containing biological liquids, is the development of precise approaches for analyzing small liquid volumes. This can be achieved by either miniaturizing the resonator through the use of materials with high dielectric permittivity (e.g. sapphire) or by incorporating small liquid reservoirs into the structure that is aligned to the resonator electromagnetic field pattern with the further development of the calibration procedure. For example, the measurement cell based on the sapphire WGM resonator with a microfluidic channel, fabricated from a low-loss plastic layer and positioned on the top flat part of the cylindrical resonator, is described in [8]. Quartz resonators, which provide better thermal stability, have larger dimensions. However, they also offer other advantage [20] of being used with the microfluidic chip (MFC) [9].

Investigating the MW properties of various biological solutions/samples is important, as it can provide valuable information on potential diseases, including cancer [21]. The MFC typically consists of a low-loss plastic layer with a microfluidic channel and metal tubes for introducing the LUT [8, 9]. However, filling, cleaning, and sterilizing the channel, as well as replacing the entire MFC, is challenging. The planar resonators based techniques are usually make use of small amount of LUT filled in capillary tube (CT). This approach can also be used for placing the LUT in the WGM resonator. In the resulting structure the liquid-filled CT is inserted into a hole in the resonator [19, 22, 23]. This design combines the advantages of the MFC resonator technique—such as high-quality factor, an enclosed and small liquid volume, and the possibility of investigating liquids with high MW losses—while overcoming the difficulties related to filling, cleaning, sterilizing, and replacing the MFC. Moreover, the CT is less complex and more cost-effective compared with the MFC. Experimental investigations of a WGM quartz resonator with a CT inserted into its hole were carried out in [23]. The influence of the properties of the LUT on the spectral and energy characteristics of the resonator were observed. Investigations of glucose in water solutions using the technique have shown the potential of the structure for determining the complex permittivity of liquids.

COMSOL Multiphysics [24] models of a WGM resonator with an MFC were used to analyze the resonant structure and determine the eigenfrequency and quality factor [8, 9]. However, these models cannot be used for analyzing WGM resonators with a CT, as the asymmetry of the structure and the direct introduction of the liquid into the electromagnetic field of the resonator require consideration of the influence of the excitation source. Moreover, as was found in [23], the response of the resonator with the hole exhibits significant mode splitting in comparison with the MFC structure [8]. Therefore, averaged values of the splitted mode characteristics cannot be used, as was the case of resonators with an MFC [8, 9].

In this work, we address several challenges, proposing an approach that allows us to determine the complex permittivity of liquids based on experimental data. For the resonator with a CT in the hole structure, a procedure to analyze the splitted mode response was developed. To solve the inverse electrodynamics problem—determining the electrophysical parameters of a substance from the resonator response—we developed an accurate model for the simulation of complex permittivity values of biochemical liquids with the subsequent development of the calibration procedure. The model allows for the numerical analysis/simulation of the interaction between the liquid and the field pattern of the resonator, which enables the structural behavior of the resonator to be predicted with different liquids filled in the CT.

2. Measurement technique

2.1. Modeling results

The model was developed using the parameters of the fabricated measurement cell described in [23]. The measurement cell includes a quartz dielectric resonator with a central hole and a hole for the CT placement, a CT itself with a liquid filling system, and a pair of dielectric waveguides for the coupling of the wave (schematic of the cell is shown in figure 1(a)). The entire measurement cell is placed in an isolated enclosure with temperature stabilization provided by the Peltier elements. The structure, consisting of a quartz resonator with a hole into which a plastic CT is inserted, is modeled using COMSOL Multiphysics software (figure 1(b)) [24].

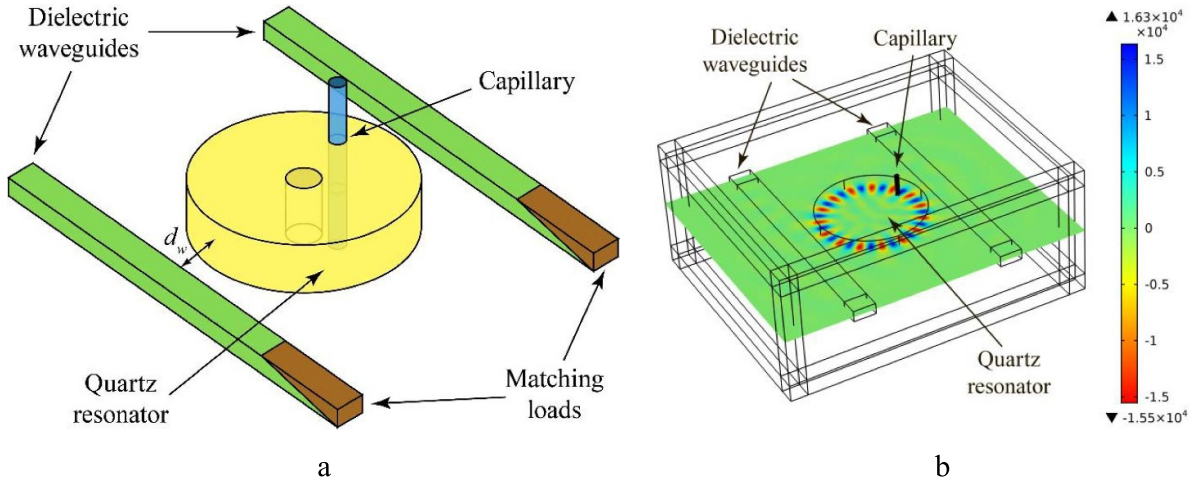

Figure 1. The WGM resonator cell: (a) schematic of the cell consisting of a quartz dielectric resonator with a central hole and a hole for the CT placement, a CT itself with a liquid, and a pair of dielectric waveguides for the coupling of the wave; (b) the model of the structure composed using the COMSOL Multiphysics software.

Quartz is an anisotropic material with permittivity in perpendicular and parallel directions to the crystal optical axis equal to $\varepsilon_\perp = 4.44\left(1 - i1.1 \cdot 10^{-5}\right)$ and $\varepsilon_\parallel = 4.63\left(1 - i8 \cdot 10^{-6}\right)$, respectively. The values were taken from [25] and refined for all WGM modes of quartz resonator in the 30-40 GHz frequency range in [9]. The quartz anisotropic axis is parallel to the resonator axis. Since the investigation was performed using a single resonance mode, the frequency dependence of quartz was not taken into account. The diameter of the resonator is equal to 24.99 mm and its height is 4.95 mm. The resonator has a cylindrical hole with a 1.01 mm diameter positioned parallel to the resonator axis and 9.75 mm from its center. As shown in figure 1(b), the hole is not positioned in the maximum of the electromagnetic field pattern, preventing a significant reduction in the quality factor of the resonator. This position was optimized to ensure that the quality factor remains high enough to allow for accurate measurements of liquid characteristic in the case of the CT filled with high-loss liquids, while also ensuring that the liquid has a sufficient influence on the resonator characteristics. This provides maximum accuracy and sensitivity for the measurements. A plastic CT with $\varepsilon = 2.38\left(1 - i \cdot 0.0077\right)$ is used for filling with the LUT. It is inserted into the resonator hole. The outer diameter of the CT is 1 mm and its inner diameter is approximately 0.5 mm. The inner diameter value was refined within the measurement accuracy by comparing the experimental data with the model calculations, resulting in a final value of 0.4918 mm, which was used in subsequent simulations.

The length of the CT is 10.5 mm. It is long enough to ensure that the edges do not affect the field distribution of the resonator. A central technological hole, used for mounting the resonator, is not included in the model, as it is located in a field-free region and thus has no influence on the characteristics of the resonator. The boundary conditions are modeled using a combination of the scattering boundary condition and an absorbing layer to effectively simulate open boundaries. The resonator is excited by two Teflon waveguides with waveguide ports located at the outer boundary of the absorbing layer.

2.2. Bare quartz resonator

To examine the impact of the waveguides on the characteristics of the resonator, preliminary studies of a bare cylindrical resonator without a hole were carried out. Figure 2(a) shows how the variation of the d_w—the distance between the resonator surface and the waveguide edge (figure 1(a))—affects the spectrum of the structure. The distance d_w is usually changed to adjust the coupling of the resonator. The lager the distance is, the weaker the coupling.

To verify the reliability of the model, the results obtained by transient analysis on resonant frequency and the quality factor of the aforementioned system are compared with those obtained by frequency-domain analysis, i.e. the eigenfrequency solver. The reliability of the latter model was previously confirmed by MFC with the quartz WGM resonator structure investigation [9] as well as by application of this resonator technique for the investigation of amino acids [20]. Since the responses of the system (figure 2(a)) are nonsymmetrical, the fitting is performed using the coupling modes approach [26] to obtain its resonance characteristics. This procedure was successfully confirmed previously for investigations of bioliquids using WGM resonators [8, 9, 27]. The quality factor dependencies on the distance between the resonator and dielectric waveguides, which were obtained by frequency-domain analysis and transient analysis for the bare quartz resonator under investigation, are shown in figure 2(b). In addition to the demonstration of good data correlation obtained by both solvers, the data in figure 2(b) can be used to estimate the weak coupling conditions. The quality factor remains almost unchanged for such a structure when increasing the distance, d_w, more than 7.5 mm.

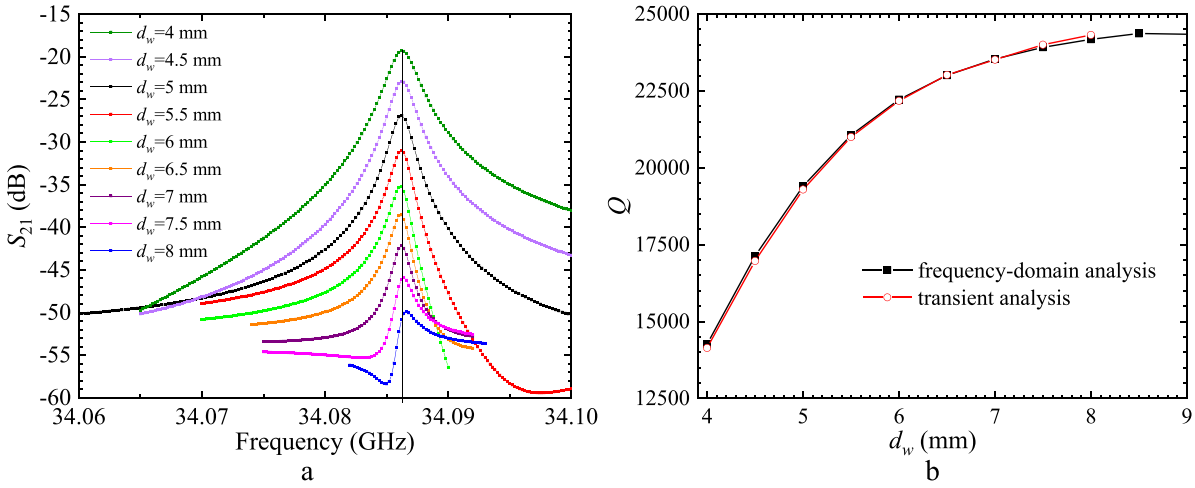

Figure 2. Modeled resonant characteristics of the bare resonator without a hole: (a) resonance responses for the different distances between resonator and waveguides d_w obtained by transient analysis; (b) quality factor dependencies on distance, d_w, obtained by frequency-domain (solid points) and transient (open points) analysis.

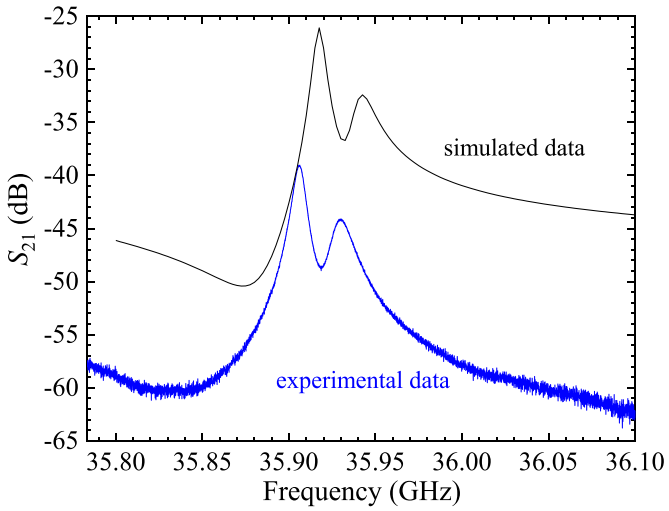

Figure 3. Experimental and simulated frequency responses of the bare resonator with a hole.

2.3. Resonator with a hole

The next step in the study is the analysis of the characteristics of the resonator with a hole for the case without the insertion of a CT. It should be noted that the position of the hole in the resonator was measured and further refined by comparing experimental results with calculated results, varying its position within the measurement error. The excitation conditions in the model were also aligned with the experimental setup using such a simulation. The responses of the resonator with a hole are shown in figure 3.

The simulated curve exhibits lower losses compared to the calculated one. This discrepancy is connected with losses in the transmission line elements (such as cables and coaxial-to-waveguide transitions) which are not taken into account in simulation. The simulated resonance lines show higher resonant frequency compared to experimental ones, although the shapes of the experimental and the simulated responses are similar to each other. The peculiarity of the response itself obtained for the resonator with a hole is a splitting of the resonances, unlike the response of the resonator without a hole. The lower frequency resonance has a higher amplitude and a higher quality factor while the higher frequency one exhibits the opposite behavior. This difference can be explained by the electromagnetic field pattern in relation to the hole position (figure 4). The lower frequency peak corresponds to a weaker field perturbation (the hole is situated between the field maxima, figure 4(a)), resulting in a higher amplitude and quality factor, as well as a stronger perturbation in the case of higher frequency ones. In the latter case, one of the field maxima is situated in the hole (figure 4(b)), resulting in a stronger interaction with the electromagnetic wave. This in turn leads to a lower amplitude and quality factor. However, the higher frequency resonance has a stronger influence on the substance in the hole characteristics.

2.4. Resonator with a hole filled with a CT

As was mentioned above the shapes of the experimental and the simulated responses of the resonator with a hole are similar to each other. This indicates good agreement between the simulated and measured absolute values of quality factor of resonator with air-filled hole. This peculiarity can be used for refining the inner diameter of the CT. The dependence of the simulated average quality factor (open circles) of the resonator with an air-filled CT on its inner diameter, along with the experimental value (solid square), is shown in figure 5. The average quality factor Q_{aver} was determined as the mean value of the quality factors of both splitted resonances.

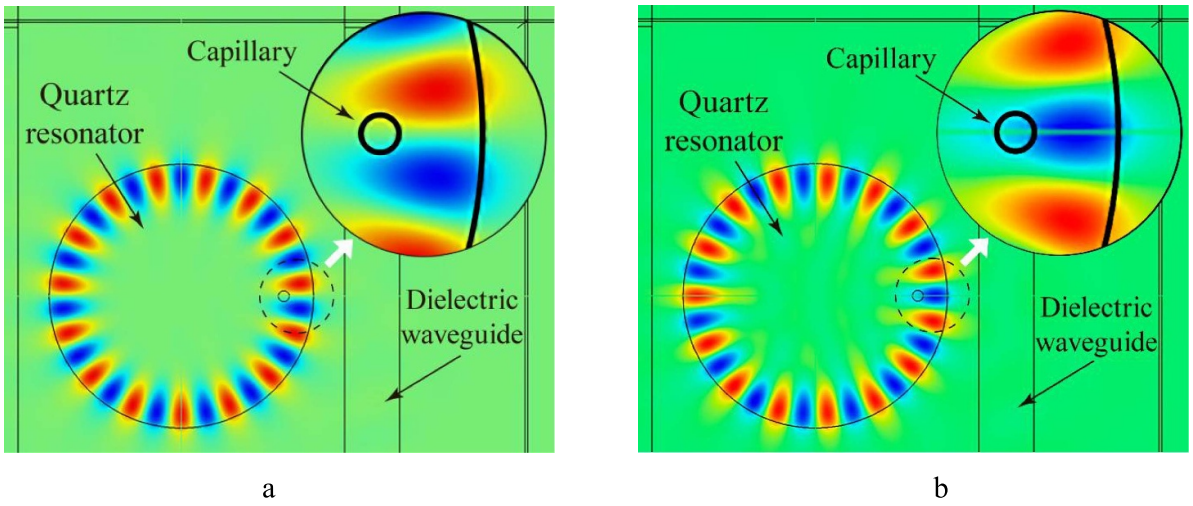

Figure 4. Electromagnetic field patterns of splitted mode resonances for: (a) a lower frequency resonance with a weak field perturbation; (b) a higher frequency resonance with a relatively high field perturbation.

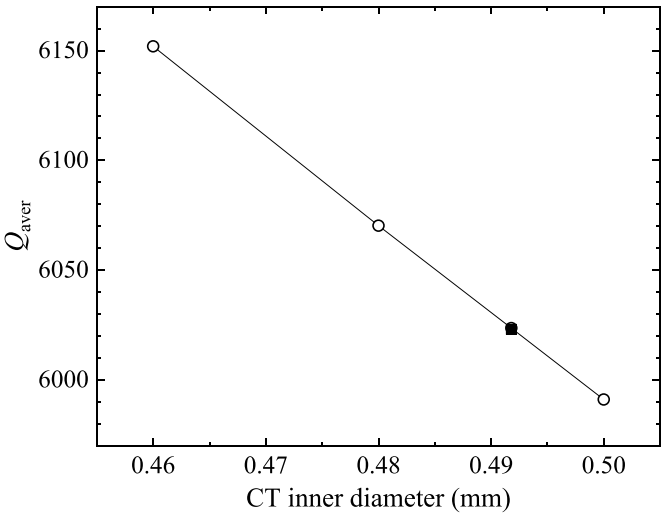

Figure 5. Dependence of the simulated average quality factor of the resonator with an air-filled CT (open circles) on its inner diameter, along with the experimental value (solid square).

The calculated dependence of the average quality factor on the CT inner diameter is linear and the experimental value corresponds to a diameter of 0.4918 mm.

2.5. Resonator with a hole filled with a CT containing a liquid of known properties

The CT fabricated from low-loss plastic ($\varepsilon = 2.38\,(1 - i \cdot 0.0077)$) has the following dimensions: length of 10.5 mm and inner diameter of 0.5 mm. The total liquid volume in the CT is equal to about 2 μl, while the volume of the liquid interacting with the electromagnetic field is approximately 1 μl. To refine the CT dimensions and ensure that the model accurately reflects the real structure, a series of experiments were carried out with a CT filled with liquids of known properties. To minimize errors in determining the permittivity, for example errors caused by CT inner diameter variations due to manufacturing imperfections, the relative changes in the resonance frequency and inverse quality factor of the structure with a CT filled with the liquid under investigation were analyzed in relation to those for a structure with a CT filled with air.

The measured and simulated frequency shift and changes in the inverse quality factor relative to the air-filled CT are presented in table 1. The permittivity of ethanol, methanol, and water for simulation were taken from [28]. The resonance frequency shift and changes in the inverse quality factor were calculated for both peaks of the split mode resonances.

As mentioned earlier, the higher frequency resonance reflects a stronger interaction with the electromagnetic field pattern compared to the lower frequency peak. The interaction with LUT reveals broadening of both peaks and the higher liquid absorption leading the broader peaks. The investigation of water solutions results a significant broadening of the resonance peaks compared to the air filled CT. The lower quality factor splitted resonance remains strong 'overlapping' with higher frequency resonance. It is therefore impossible to determine the resonant parameters of higher frequency resonance peak with sufficient accuracy for liquids with high MW absorption, such as water (table 1). The lower frequency peak has a higher quality factor as a result of a weaker interaction with the electromagnetic field pattern (figure 4(a)) and demonstrates good agreement between the measured and simulated data (table 1). In this respect, the lower frequency resonance can be used for the further permittivity determination of the LUT filled in the CT.

3. Determination of substance permittivity

A special calibration procedure was developed to determine the permittivity of the LUT for the sapphire and quartz WGM resonators with an MFC [8, 9]. We developed a similar procedure for the WGM resonator with a CT. A nomogram chart was plotted by simulating the structure with a discrete variation of

Table 1. Comparison of the measured and simulated resonance frequency shift and changes in the inverse quality factor of the resonator with a CT filled with ethanol, methanol, and water in relation to an air-filled CT.

Lower frequency resonance				
	Resonance frequency shift (MHz)		Changes in inverse quality factor	
Liquid under test	Experiment	Simulation	Experiment	Simulation
Ethanol	2.34	2.10	$3.03{\cdot}10^{-6}$	$5.19{\cdot}10^{-6}$
Methanol	3.60	3.00	$3.19{\cdot}10^{-5}$	$3.15{\cdot}10^{-6}$
Water	6.29	5.77	$1.91{\cdot}10^{-4}$	$1.91{\cdot}10^{-4}$
Higher frequency resonance				
	Resonance frequency shift (MHz)		Changes in inverse quality factor	
Liquid under test	Experiment	Simulation	Experiment	Simulation
Ethanol	6.93	6.70	$1.22{\cdot}10^{-4}$	$8.39{\cdot}10^{-5}$
Methanol	7.4	10.23	$2.72{\cdot}10^{-4}$	$3.25{\cdot}10^{-4}$
Water	—	—	$1.10{\cdot}10^{-4}$	—

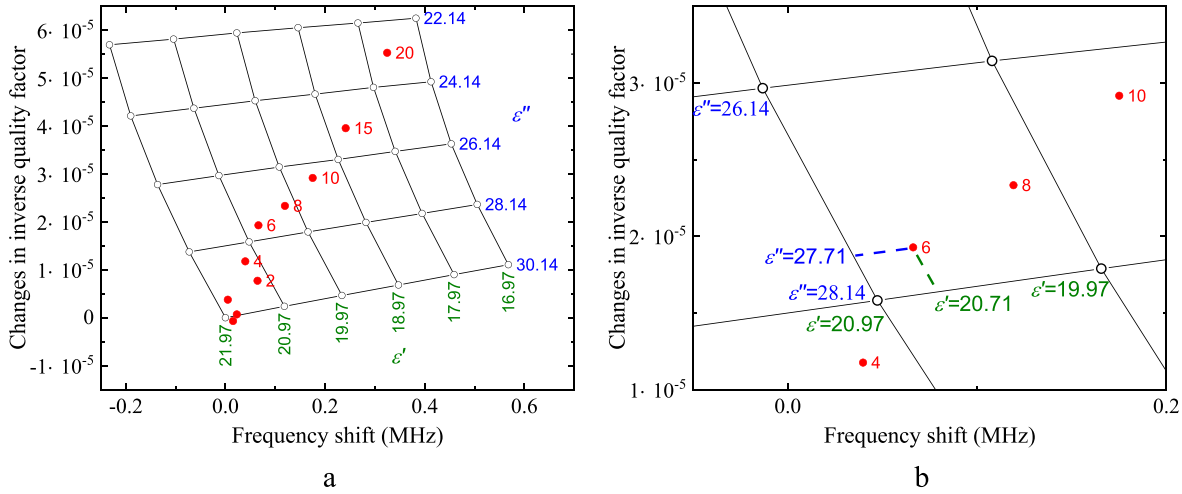

Figure 6. Nomogram chart. (a) Calculated resonant frequency shift and changes in the inverse quality factor (open points) for a CT filled with model substances for which the real and imaginary parts of the permittivity are varied. The solid points show the experimentally obtained data for different glucose concentrations in water solutions. (b) Magnified view explaining graphical determination of the real (20.71) and the imaginary (27.71) permittivity parts of the 6% glucose in water solution experimental point.

the imaginary part of a calibration liquid permittivity filling the CT, while keeping the real part constant, and vice versa (open points in figure 6). The real part of the permittivity was varied from 21.97 to 16.97 in steps of 1 and imaginary part from 22.14 to 30.14 in steps of 2. For example, the lower line in figure 6 was obtained by simulation the structure using the real part of calibration liquids permittivity set to 21.97, 20.97, 19.97, 18.97, 17.97 and 16.97 while keeping the imaginary part constant at 30.14. The nomogram chart represents relation of the frequency shift and changes in inverse quality factor with respect to real and imaginary parts of permittivity. The measured resonant frequency shift and changes in the inverse quality factor of the structure with a CT filled with different glucose concentrations in water solutions (0.25%, 0.5%, 1%, 2%, 4%, 6%, 8%, 10%, 15%, and 20%) are plotted on the nomogram chart (solid points) in relation to those of the structure with a water-filled CT. For example, for a 6% glucose solution point the real part of the permittivity was determined to be 20.71 (indicated by the green dashed line in figure 6(b)) and the imaginary part was 27.71 (indicated by the blue dashed line in figure 6(b)). The complex permittivity value for each concentration of glucose can be derived from the chart using either a graphical method (dashed lines in figure 6(b)) or by code using linear equations from the points that are closest to the experimental ones.

The values $\varepsilon' = 21.97$ and $\varepsilon'' = 30.14$ correspond to the complex permittivity of water at the studied frequency.

The complex permittivity dependencies on the concentrations of glucose in water solutions extracted from the measurement data, which were obtained using a WGM resonator with a CT, are shown in figure 7. For comparison, the dependencies of the real and imaginary parts of the permittivity on the concentrations of glucose, which were obtained using a quartz WGM resonator with an MFC [9], are depicted by the dashed

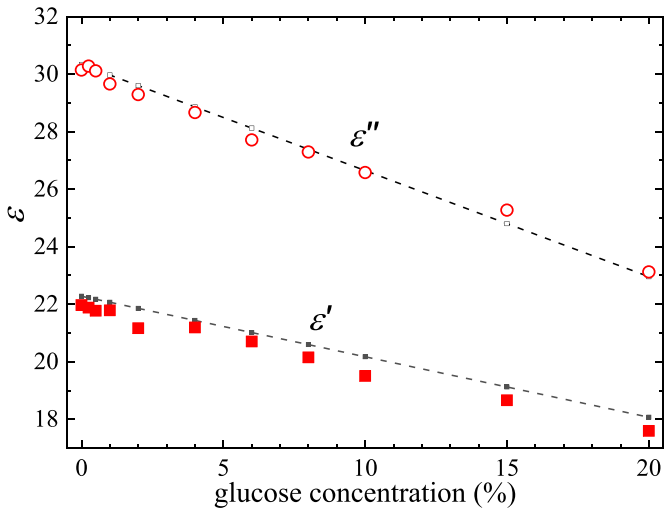

Figure 7. Real (solid points) and imaginary (open points) parts of permittivity dependencies on the concentration of glucose in water solutions at a frequency of 35.89 GHz. The data, obtained in [9] using a quartz WGM resonator with an MFC at a frequency of 35.65 GHz, are represented by the dashed line.

lines. It should be noted that there is a small systematic shift of the results caused by the difference in measurement frequencies: 35.89 GHz in the case of the CT structure and 35.65 GHz in the case of the MFC. The data obtained using both the WGM resonator with an MFC and the WGM resonator with CT methods are in good agreement.

The results of figure 7 reveal prospects for the investigation of bioliquids and solutions using the new approach represented by a WGM resonator with a CT. The relative accuracy for determining the complex permittivity values of glucose in water solutions is about 2.0% for the real part and 1.5% for the imaginary part. The accuracy of the quartz WGM resonator using the MFC technique is 0.7% and 0.4%, respectively [9]. However, the resonator with a CT structure offers several advantages: easy CT replacement, cleaning, and sterilizing with an almost equal amount of LUT. Another important aspect is that the CT is inexpensive and can be easily manufactured compared to the MFC.

4. Conclusion

A novel approach for obtaining the complex permittivity of bioliquids and solutions in the MW range using a WGM resonator with a CT in a hole of the resonator was successfully demonstrated using our developed calibration procedure. The permittivity values of glucose in water solutions, which were obtained by applying the calibration procedure, are in good agreement with the data obtained by a WGM resonator using the MFC technique. It was shown that the system allows highly sensitive monitoring changes in the concentration of substances in water solutions at small volumes (submicroliter level). The approach enables the contactless determination of the permittivity of the liquids in the MW range with several advantages. These include the simple replacement of the CT with a LUT as well as CT cleaning and sterilizing, which is especially important for the investigation of biological substances.

Data availability statement

All data that support the findings of this study are included within the article (and any supplementary files).

Acknowledgments

The authors are grateful for a research grant from the German Research Foundation (DFG) (Project VI 456/4). The work was performed within the framework of the Agreement for Cooperation between Forschungszentrum Jülich GmbH, Germany, and the O. Usikov Institute for Radiophysics and Electronics, National Academy of Science of Ukraine.

ORCID iDs

Alexey I Gubin 0000-0002-8400-242X
Irina A Protsenko 0000-0002-0640-110X
Alexander A Barannik 0000-0003-2687-2205
Svetlana A Vitusevich 0000-0003-3968-0149

References

[1] Chen L F, Ong C K, Neo C P, Varadan V V and Varadan V K 2004 *Microwave Electronics: Measurement and Materials Characterization* (Wiley)
[2] Piuzzi E, Merla C, Cannazza G, Zambotti A, Apollonio F, Cataldo A, D'Atanasio P, De Benedetto E and Liberti M 2013 A comparative analysis between customized and commercial systems for complex permittivity measurements on liquid samples at microwave frequencies *IEEE Trans. Instrum. Measur.* **62** 1034–46
[3] Keysight Application Note 5989-2589EN Basics of measuring the dielectric properties of materials
[4] Jiang X, Qavi A J, Huang S H and Yang L 2020 Whispering-gallery sensors *Matter* **3** 371–92
[5] Wei Y and Sridhar S 1989 Technique for measuring the frequency-dependent complex dielectric constants of liquids up to 20 GHz *Rev. Sci. Instrum.* **60** 3041
[6] Little C A E, Stelson A C, Orloff N D, Long C J and Booth J C 2019 Measurement of Ion-pairing interactions in buffer solutions with microwave microfluidics *IEEE J. Electromagn. RF Microw. Med. Biol.* **3** 184–90
[7] Nikolic-Jaric M, Romanuik S F, Ferrier G A, Bridges G E, Butler M, Sunley K, Thomson D J and Freeman M R 2009 Microwave frequency sensor for detection of biological cells in microfluidic channels *Biomicrofluidics* **3** 034103
[8] Gubin A I, Barannik A A, Cherpak N T, Protsenko I A, Offenhaeusser A and Vitusevich S 2015 Whispering-gallery-mode resonator technique with microfluidic channel for permittivity measurement of liquids *IEEE Trans. Microw. Theory Technol.* **63** 2003–9
[9] Gubin A I, Protsenko I A, Barannik A A, Vitusevich S, Lavrinovich A A and Cherpak N T 2019 Quartz whispering-gallery-mode resonator with microfluidic chip as sensor for permittivity measurement of liquids *IEEE Sens. J.* **19** 7976–82
[10] Havelka D, Krivosudský O and Cifra M 2017 Grounded coplanar waveguide-based 0.5–50 GHz sensor for dielectric

spectroscopy *2017 47th European Microwave Conf. (Eumc)* pp 950–3
[11] Gennarelli G, Romeo S, Scarfi M R and Soldovieri F 2013 A microwave resonant sensor for concentration measurements of liquid solutions *IEEE Sens. J.* **13** 1857–64
[12] Guo H, Yao L and Huang F 2016 A cylindrical cavity sensor for liquid water content measurement *Sens. Actuators A* **238** 133–9
[13] Javed A, Arif A, Zubair M, Mehmood M Q and Riaz K 2020 A low-cost multiple complementary split-ring resonator-based microwave sensor for contactless dielectric characterization of liquids *IEEE Sens. J.* **20** 11326–34
[14] Velez P, Lijuan S, Grenier K, Mata-Contreras J, Dubuc D and Martin F 2017 microwave microfluidic sensor based on a microstrip splitter/combiner configuration and split ring resonators (SRR) for dielectric characterization of liquids *IEEE Sens. J.* **17** 6589–98
[15] Jialu M, Tang J, Wang K, Guo L, Gong Y and Wang S 2021 complex permittivity characterization of liquid samples based on a split ring resonator (SRR) *Sensors* **21** 3385
[16] Chuma E L, Iano Y, Fontgalland G and Roger L L B 2018 Microwave sensor for liquid dielectric characterization based on metamaterial complementary split ring resonator *IEEE Sens. J.* **18** 9978–83
[17] Schaub D E and Oliver D R 2011 A circular patch resonator for the measurement of microwave permittivity of nematic liquid crystal *IEEE Trans. Microw. Theory Technol.* **59** 1855–62
[18] Yeo J and Lee J I 2022 High-sensitivity slot-loaded microstrip patch antenna for sensing microliter-volume liquid chemicals with high relative permittivity and high loss tangent *Sensors* **22** 9748
[19] Cherpak N, Lavrinovich A and Shaforost E 2006 Quasi-optical dielectric resonators with small cuvette and capillary filled with ethanol-water mixtures *Int. J. Infrared Millimeter Waves* **27** 115–33
[20] Gubin A I, Barannik A A, Protsenko I A, Chekubasheva V A, Lavrinovich A A, Cherpak N T and Vitusevich S 2023 Microwave characterization of aqueous amino acid solutions using the multifrequency WGM resonator technique *Biol. Chem.* **404** 229–35
[21] Grenier K, Dubuc D, Chen T, Artis F, Thomas Chretiennot M P and Fournié J-J 2013 Recent advances in microwave-based dielectric spectroscopy at the cellular level for cancer investigations *IEEE Trans. Microw. Theory Technol.* **61** 2023–30
[22] Gubin A I, Lavrinovich A A and Cherpak N T 2006 Dielectric resonators with "whispering-gallery" waves in investigations of small volume binary solutions *Ukr. J. Phys.* **51** 723–7 (available at: http://archive.ujp.bitp.kiev.ua/files/journals/51/7/510716p.pdf)
[23] Gubin A, Lavrinovich A, Protsenko I, Barannik A and Vitusevich S 2019 WGM dielectric resonator with capillary for microwave characterization of liquids *Telecom. Rad. Eng.* **78** 1651–7
[24] COMSOL Multiphysics COMSOL - Software for Multiphysics Simulation (available at: www.comsol.com)
[25] Krupka J, Tobar M E, Hartnett J G, Cros D and Floch J-M L 2005 Extremely high-Q factor dielectric resonators for millimeter-wave applications *IEEE Trans. Microw. Theory Technol.* **53** 702–12
[26] Skresanov V N, Glamazdin V V and Cherpak N T 2011 The novel approach to coupled mode parameters recovery from microwave resonator amplitude-frequency response *Proc. 41st Eur. Microw. Conf.* pp 826–9
[27] Gubin A I, Protsenko I A, Barannik A A, Cherpak N T and Vitusevich S A 2022 Single whispering-gallery-mode resonator with microfluidic chip as a basis for multifrequency microwave permittivity measurement of liquids *IEEE Trans. Microw. Theory Technol.* **70** 3310–8
[28] Barthel J M G and Buchner R 1991 High frequency permittivity and its use in the investigation of solution properties *Pure Appl. Chem.* **63** 1473–82